under a similar pumping condition, the resonance peak for the same azimuthal order of m = 53 well matches the single-mode lasing of the PT ring resonator at a wavelength of 1513 nm (Fig. 4B). The power efficiency and the lasing threshold are also similar because the introduced loss in the PT microring laser minimally affects the desired lasing mode. We also fabricated an additional PT microring laser with a different azimuthal PT modulation for the order of m = 55. Its lasing emission at 1467 nm (Fig. 4B) also agrees well with the multimode lasing spectrum of the conventional WGM laser for the same azimuthal order (Fig. 4A). It is evident that instead of altering the WGM in the microring resonator, the introduced PT gain/loss modulation selects the lasing WGM in the PT-broken phase over a broad spectral band. By changing the desired azimuthal order of the structured PT modulation, the single-mode lasing frequency can be efficiently selected. Although we demonstrated lasing for only two WGM orders, this mode selection concept is general and in principle valid for arbitrary gain spectra. In applications, the demonstrated stable single-mode lasing can be efficiently routed, using a bus waveguide through the evanescent ring-waveguide coupling, to photonic integrated circuits for on-chip signal amplification and processing.

We have demonstrated a PT microring laser by delicate exploitation of optical loss and gain. Such a microring laser is intrinsically single-mode regardless of the gain spectral bandwidth. This is because the continuous rotational symmetry of PT modulation enables the thresholdless PT symmetry breaking only for the desired mode. More important, our PT laser demonstration is a major step toward unique photonic devices such as a PT-symmetric laser-absorber that coincides lasing and anti-lasing [i.e., coherent perfect absorption (*29*, *30*)] simultaneously.

REFERENCES AND NOTES

1. D. C. Hanna, B. Luther-Davies, R. C. Smith, *Electron. Lett.* **8**, 369 (1972).
2. H. Ghafouri-Shiraz, *Distributed Feedback Laser Diodes and Optical Tunable Filters* (Wiley, New York, 2003).
3. M. T. Hill *et al.*, *Nat. Photonics* **1**, 589–594 (2007).
4. R. M. Ma, R. F. Oulton, V. J. Sorger, G. Bartal, X. Zhang, *Nat. Mater.* **10**, 110–113 (2011).
5. S. F. Liew, B. Redding, L. Ge, G. S. Solomon, H. Cao, *Appl. Phys. Lett.* **104**, 231108 (2014).
6. C. M. Bender, S. Böttcher, *Phys. Rev. Lett.* **80**, 5243–5246 (1998).
7. K. G. Makris, R. El-Ganainy, D. N. Christodoulides, Z. H. Musslimani, *Phys. Rev. Lett.* **100**, 103904 (2008).
8. S. Klaiman, U. Günther, N. Moiseyev, *Phys. Rev. Lett.* **101**, 080402 (2008).
9. A. E. Miroshnichenko, B. A. Malomed, Y. S. Kivshar, *Phys. Rev. A* **84**, 012123 (2011).
10. Y. Lumer, Y. Plotnik, M. C. Rechtsman, M. Segev, *Phys. Rev. Lett.* **111**, 263901 (2013).
11. A. Guo *et al.*, *Phys. Rev. Lett.* **103**, 093902 (2009).
12. C. E. Rüter *et al.*, *Nat. Phys.* **6**, 192–195 (2010).
13. Z. Lin *et al.*, *Phys. Rev. Lett.* **106**, 213901 (2011).
14. A. Regensburger *et al.*, *Nature* **488**, 167–171 (2012).
15. L. Feng *et al.*, *Nat. Mater.* **12**, 108–113 (2013).
16. B. Peng *et al.*, *Nat. Phys.* **10**, 394–398 (2014).
17. H. Schomerus, *Phys. Rev. Lett.* **104**, 233601 (2010).
18. G. Yoo, H. S. Sim, H. Schomerus, *Phys. Rev. A* **84**, 063833 (2011).
19. S. Longhi, *Phys. Rev. A* **82**, 031801(R) (2010).
20. Y. D. Chong, L. Ge, A. D. Stone, *Phys. Rev. Lett.* **106**, 093902 (2011).
21. M.-A. Miri, P. LiKamWa, D. N. Christodoulides, *Opt. Lett.* **37**, 764–766 (2012).
22. M. Liertzer *et al.*, *Phys. Rev. Lett.* **108**, 173901 (2012).
23. M. Brandstetter *et al.*, *Nat. Commun.* **5**, 4034 (2014).
24. M. Körbl, A. Gröning, H. Schweizer, J. L. Gentner, *J. Appl. Phys.* **92**, 2942 (2002).
25. J. Wiersig, S. W. Kim, M. Hentschel, *Phys. Rev. A* **78**, 053809 (2008).
26. A. Mizrahi *et al.*, *Opt. Lett.* **33**, 1261–1263 (2008).
27. L. Shang, L. Liu, L. Xu, *Opt. Lett.* **33**, 1150–1152 (2008).
28. A. Arbabi, Y. M. Kang, C. Y. Lu, E. Chow, L. L. Goddard, *Appl. Phys. Lett.* **99**, 091105 (2011).
29. Y. D. Chong, L. Ge, H. Cao, A. D. Stone, *Phys. Rev. Lett.* **105**, 053901 (2010).
30. W. Wan *et al.*, *Science* **331**, 889–892 (2011).

ACKNOWLEDGMENTS

Supported by Office of Naval Research Multidisciplinary University Research Initiative program grant N00014-13-1-0649. We thank Y.-L. Xu and K. O'Brien for helpful discussions.

SUPPLEMENTARY MATERIALS

www.sciencemag.org/content/346/6212/972/suppl/DC1
Supplementary Text
Figs. S1 to S3

8 July 2014; accepted 17 October 2014
Published online 30 October 2014;
10.1126/science.1258479

OPTICS

Parity-time–symmetric microring lasers

Hossein Hodaei, Mohammad-Ali Miri, Matthias Heinrich,* Demetrios N. Christodoulides, Mercedeh Khajavikhan†

The ability to control the modes oscillating within a laser resonator is of fundamental importance. In general, the presence of competing modes can be detrimental to beam quality and spectral purity, thus leading to spatial as well as temporal fluctuations in the emitted radiation. We show that by harnessing notions from parity-time (PT) symmetry, stable single–longitudinal mode operation can be readily achieved in a system of coupled microring lasers. The selective breaking of PT symmetry can be used to systematically enhance the maximum attainable output power in the desired mode. This versatile concept is inherently self-adapting and facilitates mode selectivity over a broad bandwidth without the need for other additional intricate components. Our experimental findings provide the possibility to develop synthetic optical devices and structures with enhanced functionality.

Since the early days of the laser, enforcing single-mode operation in a given arrangement has been one of the primary goals of cavity design (*1*). At first glance, one might expect these challenges to become less acute in the course of miniaturization, as the separation of resonances, or free spectral range, scales inversely with size. However, despite their smaller size, mode management in semiconductor lasers is still demanding because of their large inhomogeneously broadened gain bandwidth (*2*). In such broadband gain environments, the lasing of the desired mode does not prevent the neighboring resonances from also experiencing amplification. Consequently, additional steps must be taken to suppress the competing parasitic modes. This can be accomplished in a number of ways, as, for example, coupling to detuned external cavities (*3*), by including intracavity dispersive elements such as distributed feedback gratings or distributed Bragg mirrors (*4*–*6*), by spatially modulating the pump (*7*), or more recently by extreme confinement of light in subwavelength structures using metallic cavities (*8*–*10*). However, not all of these schemes are practically compatible with every type of resonator, and each of them introduces further demands in terms of design complexity and fabrication tolerances. Clearly, of importance will be to identify alternative strategies through which mode selection can be established not only in a versatile manner, but also without any negative impact on the overall efficiency.

A prominent class of integrated laser arrangements is based on microring resonators (*11*, *12*). By virtue of their high refractive index contrast, such configurations can support whispering gallery modes that exhibit high quality factors and small footprints, thus making them excellent candidates for on-chip integrated photonic applications. However, like many other microscale resonators, these cavities tend to support multiple longitudinal modes with almost similar quality factors throughout their gain bandwidth, while offering little control in terms of mode discrimination with conventional techniques.

CREOL, The College of Optics and Photonics, University of Central Florida, Orlando, FL 32816-2700, USA.
*Present address: Institute of Applied Physics, Abbe Center of Photonics, Friedrich-Schiller-Universität Jena, Max-Wien-Platz 1, 07743 Jena, Germany. **†Corresponding author. E-mail: mercedeh@creol.ucf.edu**

This inherent multimode operation drastically limits the prospects of these lasers for on-chip applications.

A number of studies have suggested that notions taken from parity-time symmetry—first developed within the framework of quantum field theories—can be observed and used in the field of optics (*13–27*). In general, a nonconservative optical system is considered to be PT-symmetric provided the gain-loss distribution is spatially balanced, in which case, its associated Hamiltonian commutes with the parity-time ($\mathcal{PT}$) operator (*28*). Under these conditions, the spectrum of this non-Hermitian system can be entirely real-valued, even though gain and loss are present (*13–16*, *28–30*). However, above a certain gain-loss contrast threshold, PT symmetry can be spontaneously broken, in which case the spectrum becomes partially complex (*17–23*, *31*, *32*). In this regime, some of the modes experience either gain or loss, while the rest remains neutral (*16*, *23*).

We show that PT symmetry breaking can be elegantly exploited to establish single-mode operation in inherently multimoded microring lasers. This is accomplished in a coupled arrangement of two structurally identical ring resonators, with one experiencing gain while the other provides an equal amount of loss. The key idea behind this mechanism is that the threshold of symmetry breaking depends solely on the relation between gain/loss and coupling. Whereas any active resonator can generally display single-wavelength operation when the pump power is reduced, selective breaking of PT symmetry can be used to systematically enhance the maximum attainable gain of this mode. This is possible even if a large number of competing longitudinal or transverse resonator modes fall within the amplification bandwidth of the inhomogeneously broadened active medium. Consequently, our approach naturally exhibits a type of broadband self-adaptive behavior and is, in principle, applicable to any active resonator configuration.

We consider two coupled microrings. The small structure size associated with such devices necessitates a high refractive index contrast. The interaction between two adjacent rings is mediated by the mutual overlap of their fields in the narrow region of greatest proximity, and the coupling coefficient κ determines the frequency splitting δω between mode pairs. As is well known, the free spectral range, or mode spacing, of a ring with radius R and effective group index n_g is given by $\Delta\omega = c/Rn_g$. Assuming an active medium with an inhomogeneously broadened amplification profile $g(\omega)$, each and every mode whose gain exceeds the resonator losses can lase (see schematic in Fig. 1A).

Following the equivalence between the mathematical frameworks of quantum mechanics and optics (*13*, *28*), PT symmetry can be established in photonic systems (*16*, *17*, *23*) provided that the complex refractive index distribution $n(\vec{r}) = n_R(\vec{r}) + in_I(\vec{r})$ obeys $n(\vec{r}) = n^*(-\vec{r})$, i.e., that the real and imaginary parts exhibit even and odd spatial distributions, respectively. In our coupled arrangement, this implies that the gain experienced in one ring is balanced by the loss in the other. If PT symmetry is unbroken, the modes neither decay nor grow, but rather remain neutral. By contrast, once the gain-loss contrast is increased beyond the coupling constant, this symmetry is broken and the respective modes experience gain or loss in conjugate pairs (*27*). This phase transition lies at the heart of our approach.

When two identical resonators are placed next to one another, the degeneracy between their respective modes is broken (see Fig. 1B). The frequency splitting δω of the resulting supermode doublets $\omega_n^{(1,2)}$ is directly proportional to the coupling coefficient, i.e., $\delta\omega = 2\kappa$. The resulting eigenfrequencies of such an active system can in general be complex, and their imaginary part describes amplification or attenuation. Meanwhile, in PT-symmetric arrangements, the relationship

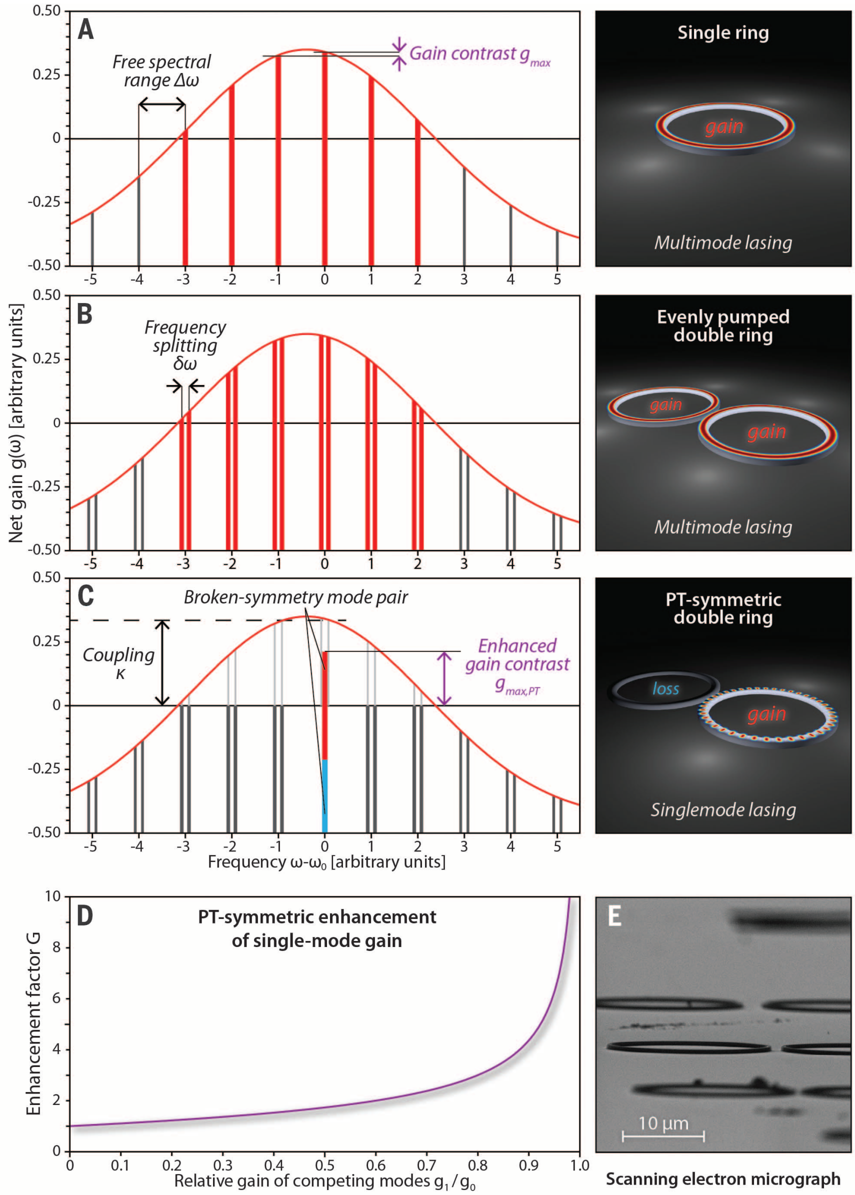

Fig. 1. Principle of mode suppression in PT-symmetric microring lasers. (**A**) An isolated ring resonator allows lasing of all longitudinal modes with positive net gain. To achieve single-mode operation, the maximum permissible gain is limited by the contrast between the resonances. (**B**) In a coupled arrangement of two identical and evenly pumped rings, the degeneracy of resonator modes is broken and mode pairs emerge. (**C**) PT-symmetric arrangement: As long as the coupling exceeds the amplification, loss and gain in the two respective rings balance each other, whereas above this threshold, PT symmetry breaking occurs. This mechanism can be exploited to enforce stable single-mode operation in otherwise highly multimoded resonators. (**D**) Enhancement factor *G* of the maximum achievable differential gain for single-mode operation in a PT-symmetric setting compared to a single active resonator. (**E**) Scanning electron microscope image of a typical set of coupled microring resonator pairs.

between eigenfrequencies and coupling is by nature different, as indicated by the following expression:

$$\omega_n^{(1,2)} = \omega_n \pm \sqrt{\kappa_n^2 - \gamma_n^2} \qquad (1)$$

Any pair of modes, whose gain-loss contrast γ_n remains below the coupling coefficient κ_n, undergoes bounded neutral oscillations. However, as soon as γ_n exceeds κ_n, a conjugate pair of lasing and decaying modes emerges. Clearly, a judicious placement of this PT threshold will allow a complete suppression of all nonbroken mode pairs in favor of a single amplified mode associated with the aforementioned conjugate pair (see Fig. 1C). As the imaginary parts of the eigenvalues diverge, degeneracy between their real parts is restored. We emphasize that even in the absence of PT symmetry, any resonator with a spectrally nonuniform gain distribution $g(\omega)$ can in principle exhibit single-mode operation, provided that the losses overcompensate the gain for all but one resonance. However, in this regime, the amplification cannot exceed the gain contrast $g_{max} = g_0 - g_1$ (see Fig. 1A). Here, g_0 refers to the gain of the principal mode, whereas g_1, to that of the next-strongest competing resonance. Obviously, this approach will impose severe constraints on the operating parameters—especially in the case of broad gain windows and/or closely spaced resonator modes, where g_{max} is very small. By contrast, in a PT-symmetric setting, the coupling κ now plays the role of a virtual loss, and all undesirable modes must fall below its corresponding threshold. According to Eq. 1, we find that in this case, the maximum achievable gain differential is given by

$$g_{max,PT} = \sqrt{g_0^2 - g_1^2} = g_{max} \cdot \sqrt{\frac{g_0/g_1 + 1}{g_0/g_1 - 1}} \qquad (2)$$

Given that $g_0 \geq g_1$, a selective breaking of PT symmetry can therefore systematically increase the available amplification for single-mode operation. The square-root behavior of this enhancement (a direct outcome of the PT symmetry breaking), as characterized by the factor $G = g_{max,PT}/g_{max}$, can provide substantially higher selectivity, especially when the initial contrast between adjacent modes is small ($g_1 \rightarrow g_0$, see Fig. 1D). This type of mode discrimination is resilient and remains valid even when PT symmetry does not exactly hold for all modes involved. On a fundamental level, the mechanism is related to the presence of an exceptional point in the system (*33*). Similar strategies have recently been proposed as means to boost the sensitivity of high-Q resonant nanoparticle detectors (*34*). The influence of deviations from ideal PT-symmetry conditions is discussed in the supplementary materials (*35*). The high mode confinement offered by our arrangement, as well as the strong coupling between rings, makes this arrangement relatively immune to local perturbations introduced by fabrication errors, nonlinearities, and/or temperature gradients (*36*).

We used electron beam lithographic techniques for the realization of active ring resonators based on InGaAsP (indium-gallium-arsenide-phosphide) quantum wells (Fig. 1E). More details on the sample fabrication are given in the supplementary materials (*35*). The gain and loss regions can be defined by selective optical pumping at 1064 nm. The gain bandwidth of the active medium spans the spectral region between 1260 and 1600 nm. In the following, the resonators were characterized by placing them within a circularly symmetric Gaussian pump beam to implement three possible configurations (single ring, evenly pumped double ring, and PT-symmetric ring arrangement). Accordingly, the effective pump powers were calculated from the geometric overlap between the active medium and the pump profile. After blocking remnants of the pump radiation by means of a notch filter, we

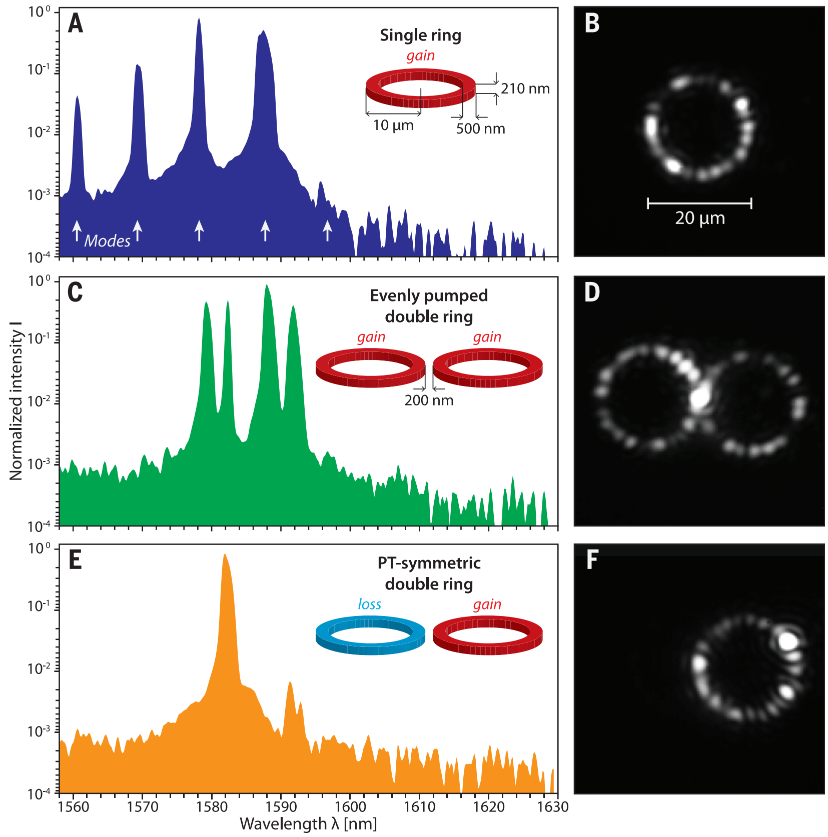

Fig. 2. Experimental observation of mode suppression by PT-symmetry breaking. (**A**) Emission spectrum of a single resonator (radius 10 µm, ring width 500 nm, height 210 nm) when exposed to a peak pump power of 4.9 mW. (**B**) Corresponding intensity pattern within the ring as observed from scattered light. (**C**) Spectrum obtained from an evenly pumped pair of such rings (4.9 mW + 4.9 mW). (**D**) The intensity pattern shows that both resonators equally contribute. (**E**) Single-moded spectrum under PT-symmetric conditions (0 mW + 4.9 mW pump). The mode suppression ratio exceeds 20 dB. (**F**) Lasing exclusively occurs in the active resonator. The single ring has a free spectral range of ~ 9.9 nm and a Q-factor of ~2×10^5. The measured linewidth of the single ring laser is ~ 0.12 nm, limited by the spectrometer resolution.

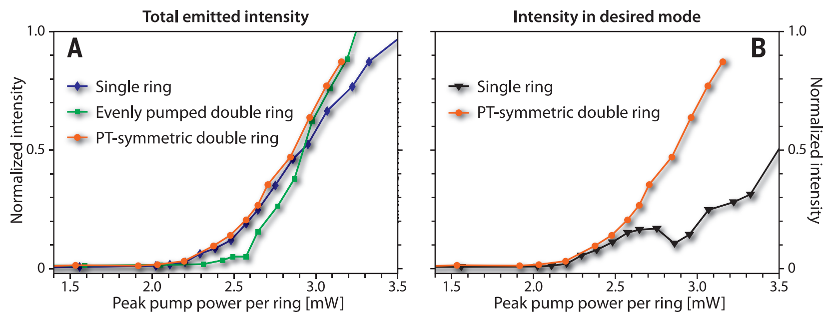

Fig. 3. Light-light characteristics. (**A**) Characteristic light-light graphs of the single, double, and PT-symmetric microring resonator arrangements shown in Fig. 2. The increased slope in the evenly pumped case is due to the doubled active area. (**B**) Spectrally resolved plots comparing the intensity emitted in the desired mode. The PT-symmetric configuration clearly offers superior performance. The onset of parasitic modes is indicated by the kinks in the single-ring graph.

simultaneously monitored the intensity profile and spectrum of the light oscillating in the microrings. Figure 2, A and B, illustrate the behavior of a single ring (radius 10 μm, ring width 500 nm, height 210 nm) when exposed to an effective peak pump power of 4.9 mW (15-ns pulses with a repetition rate of 290 kHz). Under these conditions, at least four modes contribute to lasing in the isolated ring. When two such rings are placed at a distance of 200 nm from one another, and both are exposed to the same pump power, the coupling-induced mode splitting can be seen (Fig. 2, C and D), which occurs symmetrically around the resonance wavelengths of each ring in isolation. In this coupled regime, both structures are contributing equally. Once PT symmetry is established by withholding the pump from one of the resonators (Fig. 2, E and F), lasing occurs exclusively in the active ring, where single-mode operation is now achieved. The presence of the lossy ring only serves to suppress the unwanted longitudinal modes with a contrast exceeding 20 dB. As the pump increases to very high levels, eventually the PT symmetry of other cavity modes will break, leading to multimode operation.

In the characteristic light-light curves for all three arrangements involving the 10-μm rings shown in Fig. 3A, the transition to the lasing regime, defined by the sudden onset of emission, is clearly visible. The evenly pumped double ring displays almost twice the slope of the single ring because of its larger pumped/emitting area. The PT-symmetric arrangement appears almost indistinguishable from the single ring, indicating that the presence of the lossy element does not necessarily decrease the overall efficiency. A spectrally resolved comparison of these two scenarios (Fig. 3B) reveals that the PT system offers superior performance, because the emission from the single ring includes contributions from several modes. In integrated photonic circuit applications, light from the PT-microring lasers can be optimally extracted using on-chip bus waveguides as output couplers.

Our results show that the selective breaking of PT symmetry can be used to enforce stable single-mode operation in microring laser resonators. In particular, the maximum achievable gain in PT-symmetric ring pairs can be systematically enhanced with respect to competing modes. This mechanism of mode selectivity is robust in terms of fabrication inaccuracies and can accommodate active media with wide gain spectra. Moreover, as the occurrence of PT symmetry breaking is exclusively determined by the relation between net gain and coupling, the proposed arrangement is by nature self-adapting. PT-symmetric arrangements offer superior performance in terms of efficiency. Although such designs can in principle be adopted for any type of laser cavity, they are particularly suited for the control of longitudinal modes in microring resonators, a previously challenging task. These results provide the possibility of developing classes of compact lasers that combine the advantages of multimode cavities and stable single-mode emission.

REFERENCES AND NOTES

1. A. L. Schawlow, C. H. Townes, *Phys. Rev.* **112**, 1940–1949 (1958).
2. M. Asada, A. Kameyama, Y. Suematsu, *IEEE J. Quantum Electron.* **20**, 745–753 (1984).
3. M. Fleming, A. Mooradian, *IEEE J. Quantum Electron.* **17**, 44–59 (1981).
4. H. Kogelnik, C. V. Shank, *J. Appl. Phys.* **43**, 2327 (1972).
5. M. Nakamura, K. Aiki, J. Umeda, A. Yariv, *Appl. Phys. Lett.* **27**, 403 (1975).
6. K. Iga, F. Koyama, S. Kinoshita, *IEEE J. Quantum Electron.* **24**, 1845–1855 (1988).
7. S. F. Liew, B. Redding, L. Ge, G. S. Solomon, H. Cao, *Appl. Phys. Lett.* **104**, 231108 (2014).
8. M. A. Noginov *et al.*, *Nature* **460**, 1110–1112 (2009).
9. R. F. Oulton *et al.*, *Nature* **461**, 629–632 (2009).
10. M. Khajavikhan *et al.*, *Nature* **482**, 204–207 (2012).
11. S. L. McCall, A. F. J. Levi, R. E. Slusher, S. J. Pearton, R. A. Logan, *Appl. Phys. Lett.* **60**, 289 (1992).
12. K. J. Vahala, *Nature* **424**, 839–846 (2003).
13. K. G. Makris, R. El-Ganainy, D. N. Christodoulides, Z. H. Musslimani, *Phys. Rev. Lett.* **100**, 103904 (2008).
14. R. El-Ganainy, K. G. Makris, D. N. Christodoulides, Z. H. Musslimani, *Opt. Lett.* **32**, 2632–2634 (2007).
15. S. Klaiman, U. Günther, N. Moiseyev, *Phys. Rev. Lett.* **101**, 080402 (2008).
16. A. Guo *et al.*, *Phys. Rev. Lett.* **103**, 093902 (2009).
17. C. E. Rüter *et al.*, *Nat. Phys.* **6**, 192–195 (2010).
18. S. Longhi, *Phys. Rev. A* **82**, 031801 (2010).
19. Y. D. Chong, L. Ge, A. D. Stone, *Phys. Rev. Lett.* **106**, 093902 (2011).
20. A. Szameit, M. C. Rechtsman, O. Bahat-Treidel, M. Segev, *Phys. Rev. A* **84**, 021806 (2011).
21. A. E. Miroshnichenko, B. A. Malomed, Y. S. Kivshar, *Phys. Rev. A* **84**, 012123 (2011).
22. E. M. Graefe, H. F. Jones, *Phys. Rev. A* **84**, 013818 (2011).
23. A. Regensburger *et al.*, *Nature* **488**, 167–171 (2012).
24. L. Feng *et al.*, *Nat. Mater.* **12**, 108–113 (2013).
25. M. Liertzer *et al.*, *Phys. Rev. Lett.* **108**, 173901 (2012).
26. M. Brandstetter *et al.*, *Nat. Commun.* **5**, 4034 (2014).
27. M.-A. Miri, P. LiKamWa, D. N. Christodoulides, *Opt. Lett.* **37**, 764–766 (2012).
28. C. M. Bender, S. Boettcher, *Phys. Rev. Lett.* **80**, 5243–5246 (1998).
29. T. Kottos, *Nat. Phys.* **6**, 166–167 (2010).
30. J. Schindler, A. Li, M. C. Zheng, F. M. Ellis, T. Kottos, *Phys. Rev. A* **84**, 040101 (2011).
31. B. Peng *et al.*, *Nat. Phys.* **10**, 394–398 (2014).
32. L. Chang *et al.*, *Nat. Photonics* **8**, 524–529 (2014).
33. D. D. Scott, Y. N. Joglekar, *Phys. Rev. A* **83**, 050102 (2011).
34. J. Wiersig, *Phys. Rev. Lett.* **112**, 203901 (2014).
35. More details on the breaking of PT symmetry in microring resonators, as well as additional information on the experimental techniques, can be found in the supplementary materials.
36. Y. Lumer, Y. Plotnik, M. C. Rechtsman, M. Segev, *Phys. Rev. Lett.* **111**, 263901 (2013).

ACKNOWLEDGMENTS

We gratefully acknowledge the nancial support from Army Research Office (grant W911NF-14-1-0543), NSF (grant ECCS-1128520), and Air Force Office of Scientific Research (grants FA9550-12-1-0148 and FA9550-14-1-0037). M.H. was supported by the German National Academy of Sciences Leopoldina (grant LPDS 2012-01). We thank M. Mills for helpful discussions.

SUPPLEMENTARY MATERIALS

www.sciencemag.org/content/346/6212/975/suppl/DC1
Materials and Methods
Supplementary Text
Figs. S1 to S8
References (*37*–*41*)

8 July 2014; accepted 17 October 2014
Published online 30 October 2014;
10.1126/science.1258480

GEOMORPHOLOGY

Tectonic control of Yarlung Tsangpo Gorge revealed by a buried canyon in Southern Tibet

Ping Wang,[1] Dirk Scherler,[2]*† Jing Liu-Zeng,[1] Jürgen Mey,[3] Jean-Philippe Avouac,[2]‡ Yunda Zhang,[4] Dingguo Shi[4]

The Himalayan mountains are dissected by some of the deepest and most impressive gorges on Earth. Constraining the interplay between river incision and rock uplift is important for understanding tectonic deformation in this region. We report here the discovery of a deeply incised canyon of the Yarlung Tsangpo River, at the eastern end of the Himalaya, which is now buried under more than 500 meters of sediments. By reconstructing the former valley bottom and dating sediments at the base of the valley fill, we show that steepening of the Tsangpo Gorge started at about 2 million to 2.5 million years ago as a consequence of an increase in rock uplift rates. The high erosion rates within the gorge are therefore a direct consequence of rapid rock uplift.

The topographic evolution of mountain ranges results from the competition between tectonic and erosive forces (*1*–*3*) and controls the organization of drainage and atmospheric-circulation systems (*4*–*6*). Although tectonics and erosion act in opposing directions, there may be feedbacks that couple the two (*7*, *8*). Prominent candidates for such coupling comprise the syntaxes regions (*9*, *10*), at either end of the Himalaya, where the two biggest rivers draining Tibet, the Indus and Yarlung Tsangpo, have cut deep gorges into very young metamorphic massifs (Fig. 1A) (*11*–*17*). In the so-called tectonic aneurysm model, it has been proposed that rapid incision within these gorges has thermally weakened the crust

Science
AAAS

Parity-time–symmetric microring lasers

Hossein Hodaei *et al.*

Science **346**, 975 (2014);
DOI: 10.1126/science.1258480